

Full Length Research Paper

Ocellar lamprophyre dyke bearing mineralization, Wadi Nugrus, Eastern Desert, Egypt: Geology, mineralogy and geochemical implications

Mohamed E. Ibrahim*, Gehad M. Saleh, Nazar A. Dawood and Gehan M. Aly

Nuclear Materials Authority, Egypt.

Accepted 27 August, 2010

Ocellar lamprophyre dyke (ENE-WSW) is recorded at Wadi Nugrus, Eastern Desert, Egypt. It cuts across porphyritic biotite granites and varies in thickness from 0.5 to 1.5 m and up to 3 km in length. The lamprophyre dyke is altered and it is characterized by porphyritic and panidiomorphic textures with plagioclase, olivine and augite, constituting the porphyritic phase in a fine groundmass of the same composition. Rutile, titanite, apatite, fluorite, graphite, calcite, allanite, autunite and Fe-Ti oxides are accessory minerals, while kaolinite, chlorite and epidote are secondary minerals. However, carbonitization and hematitization are common. Rounded to sub-round porphyritic and zoned ocelli with radiate or brush-like shapes are generally common and they represent physical traps for mineralization. The ocellar features are interpreted to represent the late stage of magmatic segregation or magmatic crystallization involving two immiscible magmatic liquids. Mineralogical results of altered lamprophyre samples, based on X-ray diffraction (XRD) and environmental scanning electron microscopy (ESEM), indicate the presence of secondary uranium minerals (autunite and uranophane), associated with gold, silver, nickel, atacamite, molybdenum, pyrite and zincite; moreover, the presence of kaolinite indicates a high temperature environment. The mixing of volatile fluids with meteoric water and fluid-wall rock interaction result in changes of pH and oxygen activity and deposition of base metals in reducing environs (graphite and pyrite). Precipitation of hematite probably decreased the pH of the solution and rising acidic fluids. The sudden change in pH and temperature of the fluids leads to destabilization of base metal complexes favoring their deposition. The magma source of the Nugrus lamprophyre is determined to be between calc-alkaline and alkaline and it has HKCAB and shoshonitic nature, which may be derived from decomposition melting of such a metasomatised lithospheric mantle. Olivine is a major fractional phase to account for the rapid decrease in Ni and Fe₂O₃ and increase in SiO₂. Also, clinopyroxene fractionation is important in accounting for the positive correlations of CaO and Cr versus MgO, whereas plagioclase differentiation is insignificant according to the negative correlations between MgO and Al₂O₃ and Sr. Crystal fractionation of accessory minerals such as apatite and Fe-Ti oxides are insignificant because of the less variable P₂O₅ and TiO₂ contents.

Key words: Lamprophyre, calc-alkaline, ocelli, geochemistry, mineralization.

INTRODUCTION

Lamprophyre rocks are genetically referred to as ultramafic, mafic and/or intermediate rocks that intrude the basement at shallow crustal levels and form dykes and/or sills. Furthermore, lamprophyres are porphyritic

rocks consisting of phenocrysts of mafic minerals and apatite, embedded in a groundmass that has the same composition of the early crystallized minerals, plus alkali feldspar and/or plagioclase. Among the early crystallized mafic minerals are phlogopite, olivine, amphibole, clinopyroxene and apatite. Microscopically, the mineralogy of lamprophyres includes ilmenite, garnet, titanite, allanite, sulfide, carbonate, zircon, thorite, monazite and other

*Corresponding author. E-mail: dr_mahmadi@yahoo.com.

minor phases. Extensive reviews of lamprophyric rocks can be found in Bergan (1987) and Rock (1991).

Petrographic relationships observed in both lamprophyres and lamproites suggest that such rocks were crystallized from volatile-rich magma produced from a metasomatized mantle source (Ringwood, 1990). The calcite-rich lamprophyre dikes, with primary magmatic calcite ocelli and dike-margin calcite veins, provide a unique setting that have been used to compare two methods of interpreting the forces associated with dike intrusion, crystallization and tectonic deformation (Turner, 1953).

Most of the basic dykes in Egyptian Precambrian rocks are non-mineralized and have not attracted exploration geologists. However, the lamprophyre dykes at Wadi Abu Rusheid (0.5 km northwest of the study area) represent a chemical and physical traps for polymetalization, where they play an important role as a heat source, which has led to remobilization of U, REE and some base metals (for example, Zn, W, Pb, Ag, Ni, Au and Cu in NNW-SSE and E-W directions) at Abu Rusheid cataclastic rocks (Ibrahim et al., 2006, 2007a, b, c).

In the current research, major and trace elements for the lamprophyres have been analyzed and interpreted. These geochemical data have been used to study the petrogenesis of those lamprophyres dykes and to provide constraints on the tectonic evolution and mineralization at Wadi Nugrus, Eastern Desert, Egypt.

OCCURRENCE AND PETROGRAPHIC FEATURES

Regional geology

The tectonostratigraphic sequence of the Precambrian rocks of Abu Rusheid area (Figure 1) is arranged from base to top as follows: (i) Ophiolitic *mélange*, consisting of ultramafic rocks and layered metagabbros set in metasediment matrix; (ii) Cataclastic group, consisting of protomylonites, mylonites, ultramylonites and silicified ultramylonites; (iii) Granitic rocks and (iv) Post-granitic dykes and veins (Ibrahim et al., 2004).

The cataclastic rocks of Abu Rusheid area are cross-cutting by two shear zones with a mean direction of NNW-SSE and E-W. Lamprophyre dykes bearing mineralization (U, REEs, Zn, Cu, Pb, W and Ag) were emplaced along the two shear zones (Ibrahim et al., 2006, 2007).

Abu Rusheid granitic pluton is elongated in NW-SE direction with a length of ~3.5 km and thinning in NE-SW direction with a width of ~1.6 km. Granitic rocks are characterized by porphyritic biotite granites from the NW side and followed by deformed biotite granites and two mica granites toward the SE part (Ibrahim et al., 2004). Porphyritic biotite granites are characterized by grey color and coarse-grained with K-feldspar crystals up to 2 cm in length. Biotite granites can be classified into two phases:

high deformed and low deformed biotite granites. They are medium- to coarse-grained, jointed and show different shades of colors that range from brown at the periphery to creamy in the center of the pluton; small xenoliths of mafic rocks up to 1 × 0.5 m, as well as roof pendants of mylonites that were recorded. Post-magmatic activities are represented by lamprophyres, pegmatites and quartz veins.

Local geology

The study area was mapped at 1:2000 scale (Figure 1), whereas the porphyritic-biotite granites are highly sheared and dissected by three sets of strike-slip faults with the main direction of NE-SW, ENE-WSW and NW-SE. The porphyritic-biotite granites carry cataclastic xenoliths, while the ENE-WSW fault set was intruded by lamprophyre dykes. Lamprophyre dyke at Wadi Nugrus cuts porphyritic-biotite granites and a small part of ophiolitic *mélange* and has a width that does not exceed 1.0 m and a length up to 3.0 km. However, it has sharp vertical and highly irregular contacts with the porphyritic-biotite granites (Figures 2a and b).

The NNW-SSE lamprophyre dyke which cross-cuts the hot cataclastic rocks (poly-mineralized) at Abu-Rusheid area, stopped at ENE-WSW lamprophyre dyke at Wadi Nugrus (Figure 1). So, most of the migrated mineralization from hot cataclastic rocks along the shear zone toward the SSE direction were accumulated at the wall zone of Nugrus ENE-WSW lamprophyre dyke. Variations in grain size and color indicate high-temperature alteration (chill margins) at dyke margins.

The Nugrus ENE-WSW lamprophyre dyke is fine to medium grained, greenish with olivine and clinopyroxene in sub-rounded globular features (ocelli) in fine grained (aphanitic) groundmass; whereas in thin section, the lamprophyre displays distinct inequigranular and porphyritic textures (Figures 2c and d). The modal percentage of macrocryst (xenocrysts and phenocrysts) minerals range between 5 and 10%. Xenocrysts, mainly of olivine and clinopyroxene, are larger in size and are extensively fractured.

An important feature of these xenocrysts is extensive deuteric alteration, which is practically absent in groundmass phase minerals. Groundmass often shows fluidal defined by magmatic orientation of clinopyroxene and plagioclase. The calcite present in the lamprophyre is magmatic based on the petrographic intergrowths of calcite ocelli and other minerals observed in thin section (Figure 2e).

The ocelli consist mainly of rounded spots with radiate or brush-like feldspars or of quartz and feldspar (orthoclase) in which there has been progressive crystallization from the margins towards the center. A central area of quartz probably represents an original cavity that is filled at a later period. The ocellar features

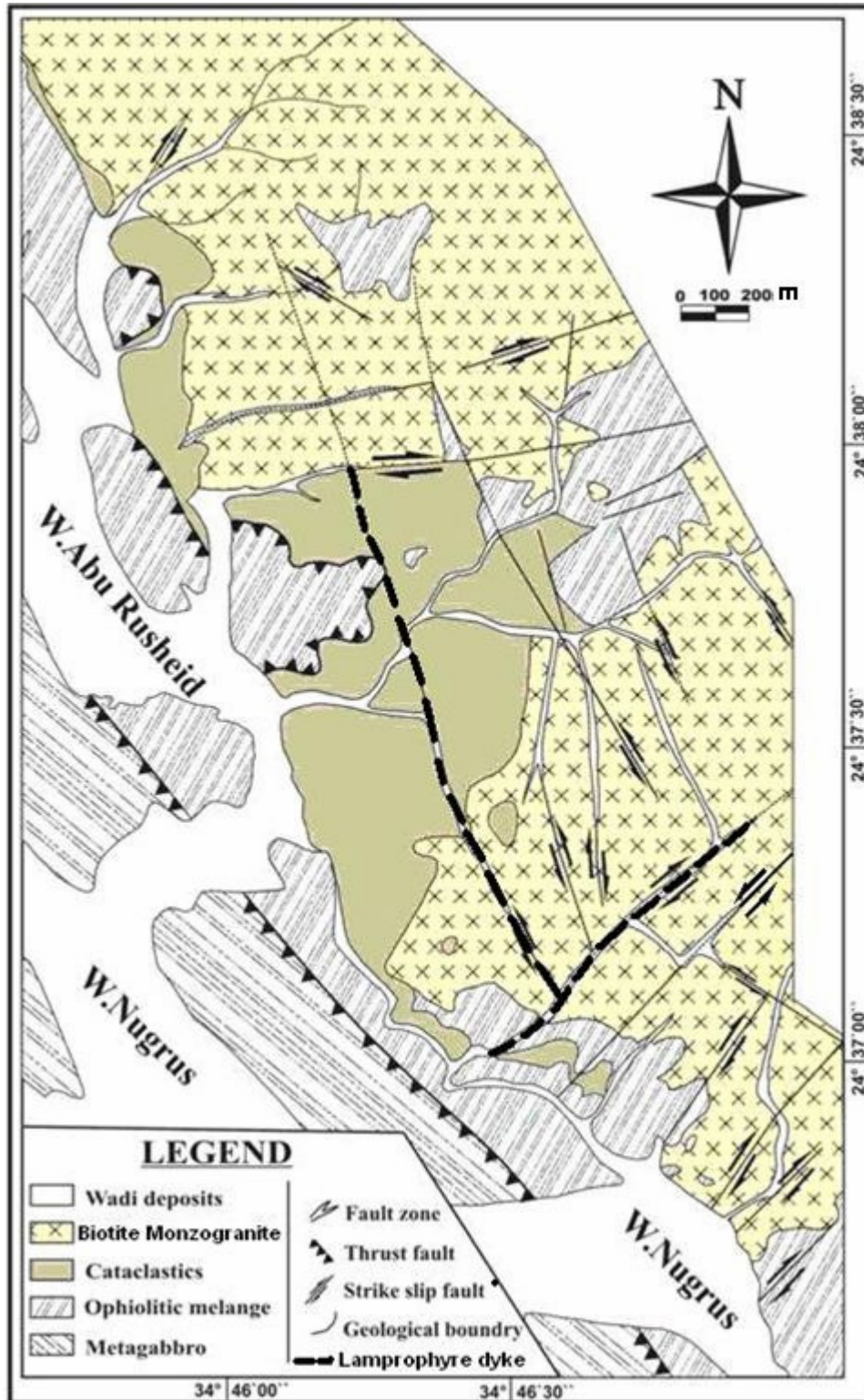


Figure 1. Detailed geologic map of Abu Rusheid area, South Eastern Desert, Egypt, after Ibrahim et al. (2004).

are believed to represent either (i) magmatic crystallization involving two immiscible liquids (Philpotts, 1976; Eby, 1980) or segregation of late stage liquid (Cooper,

1979). One of the characteristic features of the Nugrus lamprophyre is the presence of light colored segregates referred to as ocelli. They are distinctly leucocratic than

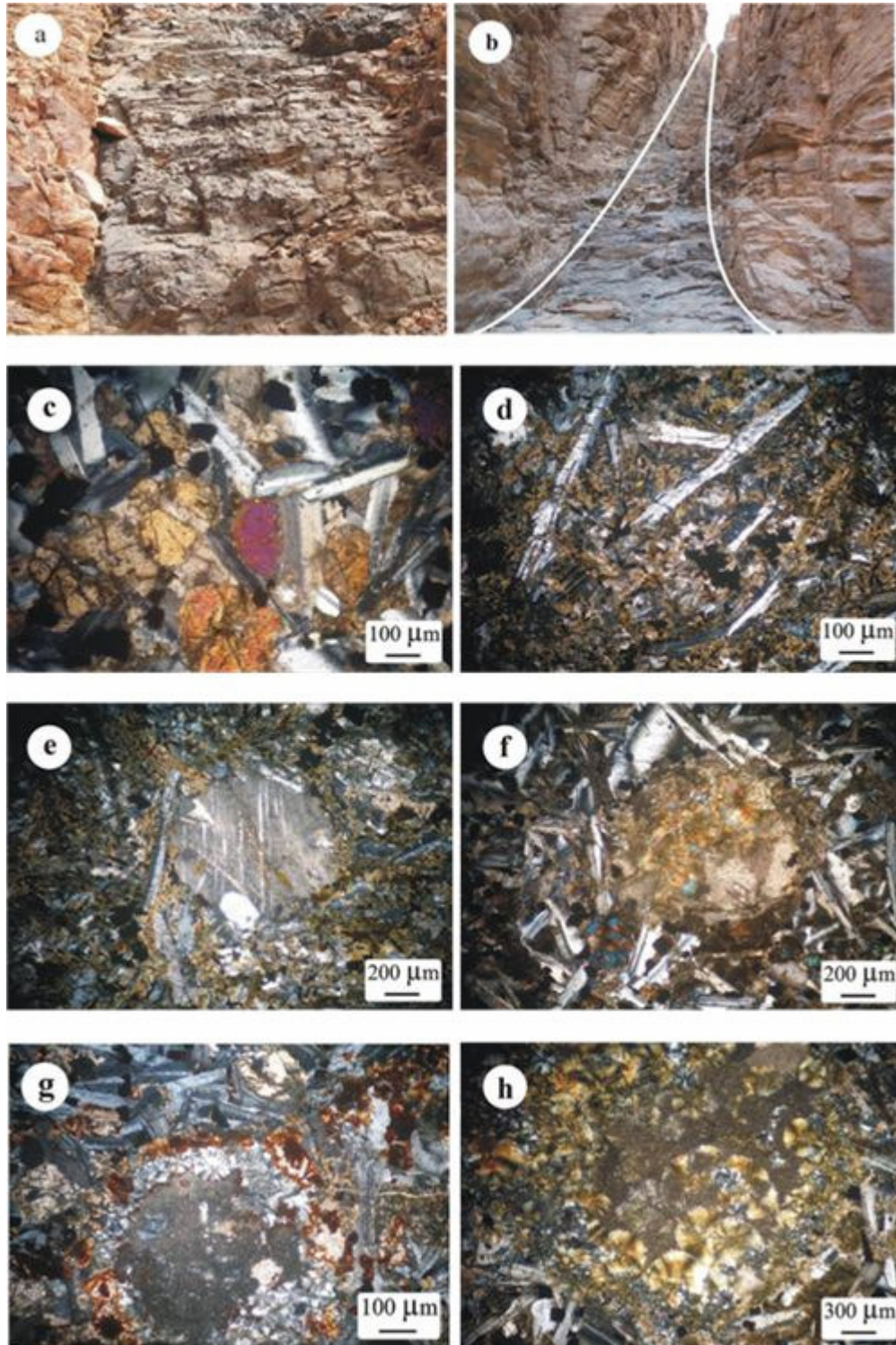


Figure 2. Lamprophyre field photos and photomicrographs showing (a and b) Sharp, straight contact between porphyritic granites and lamprophyre dyke, (c) Olivine phenocryst (partially altered and ovoid in the central part), (d) Twinned aggregates of clinopyroxene, (e) Primary calcite ocelli- intergrowth (note multiple twin sets in calcite) and (f, g and h) Ocelli (rounded) textures in *W. Nugrus* lamprophyre.

the host lamprophyre and have uniform size range of 0.3 to 0.4 cm. They are generally rounded to sub-rounded, but elongated ocelli are not uncommon (Figures 2e to h).

Groundmass in the ocellus is made of carbonate in the core that is followed outward by quartz and hematite at the margins.

Zircon, titanite, apatite, Fe-Ti oxides, sulfide, carbonates, quartz, epidote, monazite and allanite are accessory phases. Moreover, the rocks generally underwent a low grade of alteration as a consequence of calcification, hematitization and sericitization.

The early minerals comprise olivine, hornblende, clinopyroxene and apatite. The crystallization order in the paragenesis shows that the early magmatic has lesser amounts of hornblende, Fe-Ti oxides, monazite and zircon. In the late magmatic stage, the same minerals are crystallize in low proportions, along with alkali feldspar, oligoclase, occasionally quartz, Fe-Ti oxide, titanite, carbonate and other accessory phases.

Geochemistry

Analytical methods

Major and trace elements for twelve samples from Wadi Nugrus lamprophyre dyke (Table 1) were analyzed at the Laboratories of Nuclear Materials Authority, Cairo, Egypt, by X-ray fluorescence spectrometry. Detection limits were 0.01% for major elements and 5 ppm for trace elements, except where a different value is indicated in brackets.

Geochemical characteristics

Nugrus lamprophyre dyke wide span ranges of SiO₂ (44.00 – 52.00), MgO (1.30 – 5.10), CaO (1.60 – 10.00) and Fe₂O₃ (4.90 – 17.70) with Mg numbers of 43 - 59, similar to potassium-rich lamprophyres were reported by Chang et al. (1998). They are mainly calc-alkaline and partially alkaline according to Rock's (1987) classification scheme in a K₂O versus SiO₂ diagram (Figure 3 a). Nugrus lamprophyre samples plot in the field of calc-alkaline-alkaline types in V/Cr versus Nb/Pb diagram (Figure 3b), compositionally lie within the field of lamprophyres (Figure 3c). Although the clinopyroxene in the lamprophyre of the study area is poorer in Na₂O, the samples plot in calc-alkaline field is discriminately in a diagram using MgO/Fe₂O₃ vs. SiO₂/TiO₂ (Figure 3d).

The geochemical data presented in Table (1) shows that all of the samples are poor in potassium. On a conventional Harker diagram of K₂O vs. SiO₂ (Figure 4a), the samples define a rough trend between 44 and 54% of SiO₂ at low KO₂ and lie almost totally within the shoshonite and high KCAB fields defined by Peccerillo and Taylor (1976). However, in the CaO versus Al₂O₃ diagram (Figure 4b), the lamprophyre samples are occupied by the transitional groups III and IV. Several occurrences of this transitional group are minettes. Major elements similarity with the orogenic group III suggests that the source of the lamprophyre samples was probably affected by an orogenic event before the generation of parental magma. The mg # is intermediate and varies from 43 to 59, which is also typical of mica-lamprophyres

(Lloyd et al., 1985; Cesborn et al., 1993). On the (K₂O + Na₂O) – SiO₂ classification diagram by Le Maitre et al. (1989), all lamprophyre samples fall in the field of gabbro, foid gabbro and foid diorite (Figure 4c).

Systematic correlations between MgO vs. major oxides and trace elements suggest an important role of fractional crystallization (Figure 5); whereas positive correlations between MgO vs. TiO₂, P₂O₅ and Ba and negative correlations of MgO vs. Al₂O₃, CaO and SiO₂ are observed (Figure 5).

The systematic variation trends between MgO and the major and trace elements indicate magma evolution. However, olivine is a major fractional phase to account for the rapid decrease in Ni and Fe₂O₃ and an increase in SiO₂ (Figure 5). As can be seen in Figure 5, clinopyroxene fractionation is also important to account for the positive correlations of CaO and Cr vs. MgO, whereas plagioclase differentiation is insignificant according to the negative correlations between MgO and Al₂O₃ and Sr. Crystal fractionation of accessory minerals such as apatite and Fe-Ti oxides are insignificant because of the less variable P₂O₅ and TiO₂ contents. As a whole, a fractional mineral assemblage of OL + CPX ± PL can roughly explain the chemical variation trends in the calc-alkaline-alkaline lamprophyres in Wadi Nugrus.

The primitive mantle-normalized patterns of incompatible elements (Figure 6) show characteristic enrichments in Rb, Zr, Nb and Pb, while depletion in Sr, Ni and Cr are typical of subduction-related magmas. Such characteristics exclude a typical peridotitic mantle source. A strong negative spike at Sr is another relevant feature of the primitive mantle-normalized patterns.

Mineralization

Methodology

For studying the mineralogy of lamprophyre dyke under investigation, the study involved the separation of some heavy minerals fractions using magnetic isodynam operated at different current intensities. The washed heavy mineral fractions and also some slaps of lamprophyre are examined by the Environmental Scanning Electron Microscope (model Philips XL 30 ESEM) supported by a semi-quantitative energy dispersive unit (EDX). These analyses were carried out in the laboratories of the Nuclear Materials Authority (NMA), Cairo, Egypt. The analytical condition was 25 to 30 Kv accelerating voltages, 1 to 2 mm beam diameter and 60 to 120 second counting times. Minimum detectable weight concentration is from 0.1 to 1 wt%. Precision is well below 1.5, while the relative accuracy of quantitative result is 2 to 10% for elements Z > 9 (F) and 10 to 20% for the light elements B, C, N, O and F. The results of mineralogical study are listed in Figures 7 and 8 and Table 2.

Secondary uranium minerals

(1) Uranophane occurs as radiating soft grains with yellow colors, monoclinic calcium uranyle silicate and common in oxidation zones of most uranium minerals (Cesborn et al., 1993). The ESEM analyses show beside Ca, U and Si that some appreciable amounts

Table 1. Major oxides (wt %) and trace element (ppm) composition of Wadi Nugrus lamprophyre dyke, Southeastern Desert, Egypt.

Major oxides	1	2	3	4	5	6	7	8	9	10	11	12
SiO ₂	45.80	44.80	52.00	46.60	44.00	44.50	44.90	49.80	48.40	48.60	49.00	48.10
Al ₂ O ₃	16.60	15.10	13.60	14.30	15.00	16.20	16.10	16.70	14.90	15.10	14.60	23.00
TiO ₂	0.97	0.88	0.91	0.93	0.94	0.85	0.96	0.94	0.97	0.98	0.99	0.99
Fe ₂ O ₃	15.50	17.70	16.30	17.70	14.00	15.30	13.00	9.90	17.60	15.70	15.30	6.80
MgO	4.60	5.10	3.50	4.80	2.30	3.10	2.50	3.40	3.50	4.70	5.80	4.20
CaO	6.10	5.10	5.40	5.90	9.00	10.00	7.70	6.80	5.80	5.90	4.50	6.20
Na ₂ O	3.10	3.90	2.50	3.10	3.90	3.10	4.40	7.80	3.20	3.10	2.70	3.10
K ₂ O	1.90	2.10	1.50	1.90	1.10	1.70	1.20	1.00	1.80	1.80	1.90	1.50
P ₂ O ₅	1.50	1.60	1.70	1.60	0.40	0.50	1.90	0.40	1.70	1.70	2.10	1.80
L.O.I.	3.80	2.80	3.20	2.30	9.10	4.70	7.20	3.10	2.00	2.30	2.50	3.70
Total	99.87	99.08	100.61	99.13	99.74	99.95	99.86	99.84	99.87	99.88	99.39	99.19
C	0.63	2.6	0.7	0.3	1.5	1.8	0.9	1.2	0.8	2.2	1.1	1
Mg number	46	45	54	47	43	46	44	56	53	55	57	56
Trace elements												
Cr	76	67	69	69	308	217	69	72	56	46	63	33
Ni	40	38	43	38	136	75	43	20	19	20	22	6
Cu	20	19	20	19	32	31	20	18	18	17	17	-
Zn	157	158	116	156	139	327	116	184	172	223	227	87
Zr	690	707	772	779	168	239	772	613	572	575	507	1815
Rb	120	130	139	135	52	18	139	47	31	41	40	73
Y	80	81	92	88	28	19	92	74	69	72	64	93
Ba	769	834	796	815	246	252	796	826	856	1027	1099	172
Pb	12	9	9	7	5	6	9	13	11	14	10	10
Sr	222	211	243	234	255	256	243	232	224	219	197	10
Ga	22	23	28	22	22	20	28	28	27	21	22	36
V	338	351	297	355	279	293	297	346	328	367	361	8
Au	1.5	0.5	3	1	2	3	1	2	1	0.5	1.5	2
Nb	18	32	22	21	20	17	22	23	22	21	17	40

of Al, P, K and Na have also been detected. Moreover, minor Fe has also been detected (Figure 7a). This could be attributed to Fe proxying for Ca in a later phase of mineralized fluids interaction. This is in agreement with Heinrich (1956) who reported appreciable amounts of Fe in the chemical analyses of uranophane.

(2) Autunite occurs as yellowish soft grains with flaky

shape, whilst the ESEM analyses show ideal analyses of U, Ca and P.

Base metal minerals

Gold exhibits in globular form filling the interspaces

between olivine crystals, indicates precipitation from a colloidal system (Osman, 1999), and range from 0.5 to 3 g /ton. Both Cu and Zn are detected as impurities with Au, while silver is also detected as small nuggets within mafic grains. Pyrite occurs, as well developed cubic crystal with pale yellow color and metallic luster. The ESEM analyses of pyrite grains indicate that Ni is the

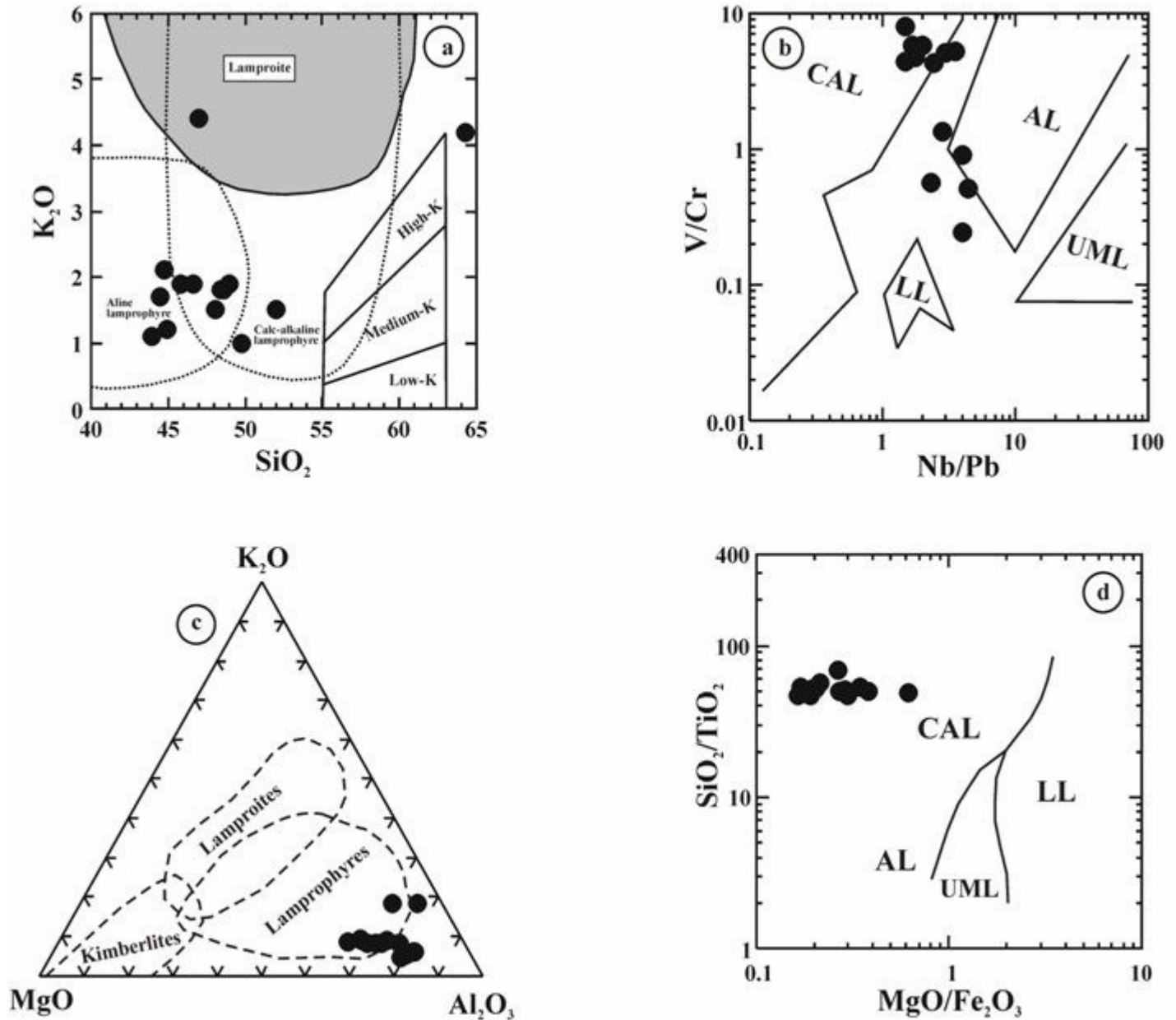


Figure 3. (a) SiO_2 vs. K_2O plots for rock classification. The lamprophyre classification scheme refers to Rock (1987), (b) V/Cr vs. Nb/Pb (AL = alkaline lamprophyre, CAL = calc- lamprophyre, LL = lamproitic lamprophyre and ULM = ultramafic lamprophyre after Rock, 1991) showing Nugrus lamprophyre plot between calc-alkaline and alkaline types, (c) Ternary plot of $\text{K}_2\text{O} - \text{MgO} - \text{Al}_2\text{O}_3$ where the study samples plot is in lamprophyre field and (d) Discrimination diagram A- $\text{MgO/Fe}_2\text{O}_3$ vs. $\text{SiO}_2/\text{TiO}_2$ showing Nugrus lamprophyre samples plot in calc-alkaline field (Rock, 1989).

main substitute for Fe^{+2} . The occurrence of pyrite induces reducing conditions, favorable for precipitation of radioactive mineralization.

Copper occurs in a rod shape with a golden yellow color, whilst the ESEM analyses of Cu show traces of S. The copper was subjected to supergene alteration and oxidation, where it converted to hydroxide (atacamite, $\text{CuCl}(\text{OH})_3$). The absence of exsolution texture indicates epithermal origin (Ramdohr, 1969) probably less than 300°C (Craig and Vaughan, 1981). Nickel is present as large grains with some Fe, while molybdenum is present as massive grains. Subsequently, the ESEM analyses show its composition as pure molybdenum with relics of Ti. Moreover, zinc converted to

zincite and occurred as silver color platy grains.

Accessory minerals

Zircon occurs as subhedral to euhedral crystals and is colorless to pale yellow in color. The ESEM analyses of zircon crystals indicate the presence of a significant amount of Zr and Si. The analyses also show a substitution of Zr by Hf, Th and U; moreover, Fe occurs as staining Fe-oxi-hydroxide. The REE concentrations in zircon crystals are always below EDX detection limit, in which fluorite

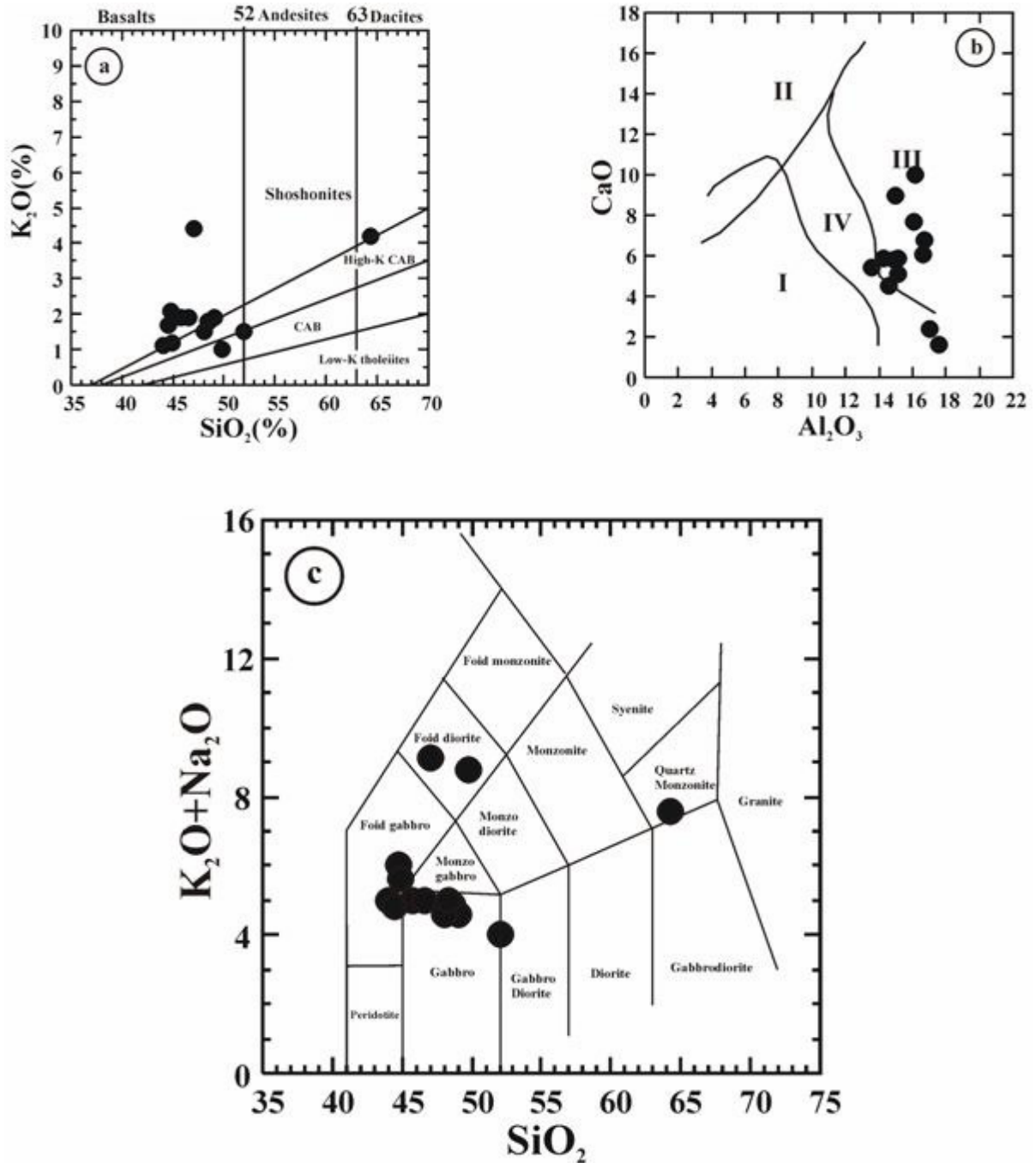


Figure 4. (a) Classification diagram for the Wadi Nugrus lamprophyre K_2O vs. SiO_2 (after Peccerillo and Taylor, 1976; ultrapotassic as defined by Foley et al., 1987), (b) Discrimination diagram (wt %) of Foley et al. (1987) applied to different groups of ultrapotassic rocks and (c) Total alkali ($Na_2O + K_2O$) versus SiO_2 (wt %) diagram (Le Maitre et al., compositional fields defined for plutonic rocks).

shows color ranges from pale violet to very deep violet. The ESEM analyses show its typical composition, whereas small amount of P appear in the analyses. The presence of fluorite accompanying the mineralization indicates that the alteration process is mainly due to hydrothermal activity.

Allanite (orthite) is a member of the epidote group, but the allanite mineral is less stable than others. It often occurs in the metamict state due to the destruction of the crystalline structure by

the alpha particle emitted. In most cases, allanite mineral is a uranium and thorium carrier and is altered to an amorphous substance product by a break down of the space lattice by radioactive emanation (Kerr, 1977). Moreover, most allanite contains some thorium up to 3% (Berry et al., 2000). The non-metamict allanite is distinguished from other epidote by their brownish color and from the metamict ones by their isotropic character (Deer et al., 1992). It occurs as tabular crystals that have

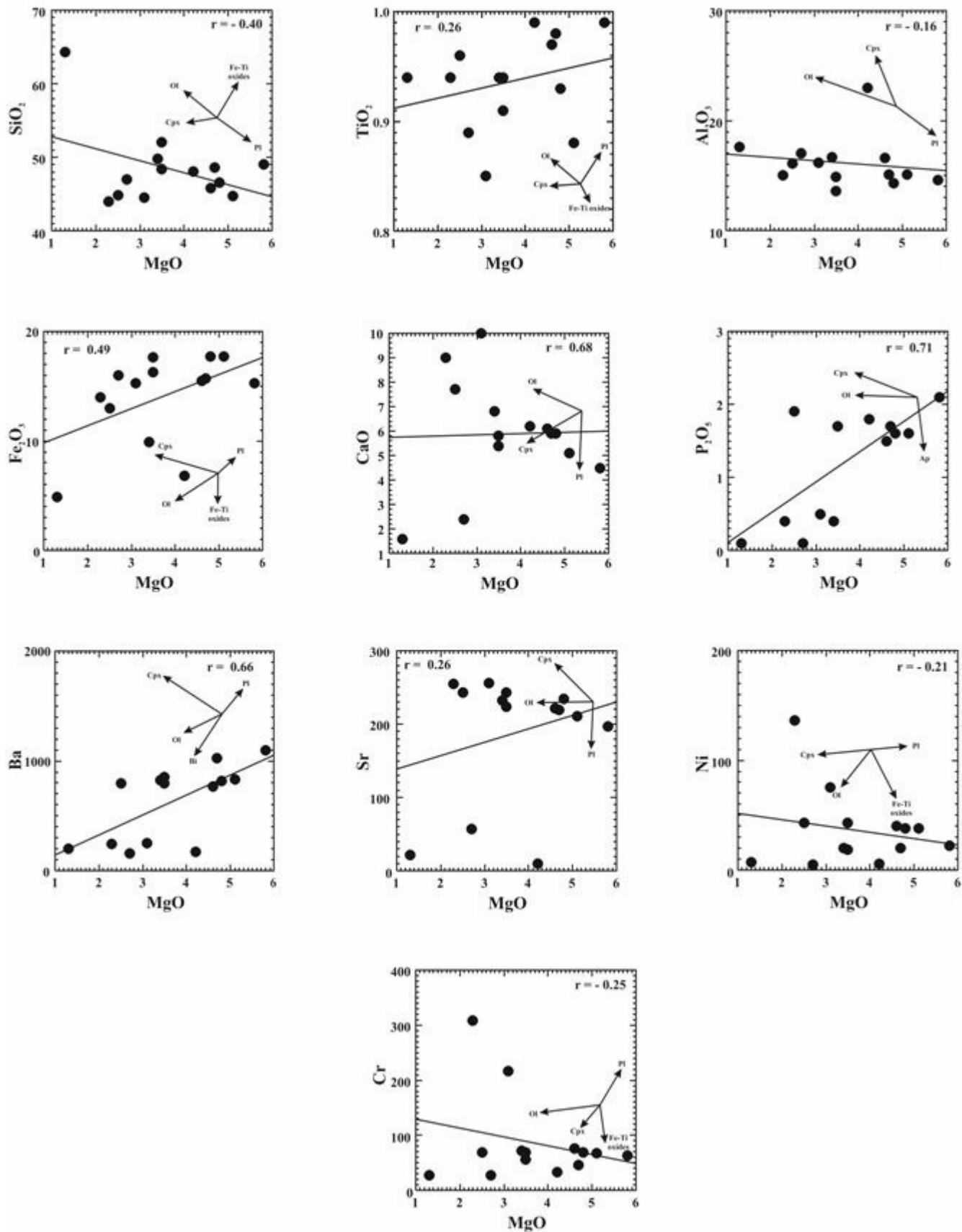


Figure 5. MgO vs. major and trace element diagrams of the Wadi Nugrus lamprophyre dyke.

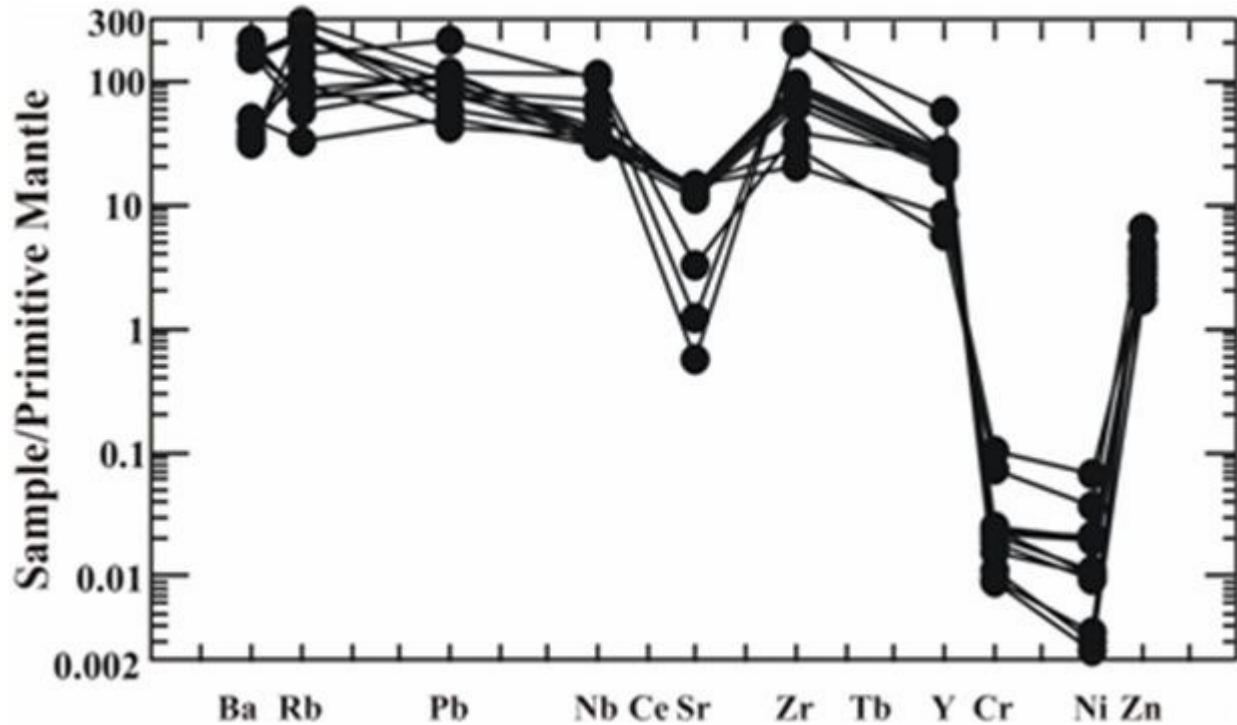


Figure 6. Primitive mantle-normalized (Sun and McDonough, 1989) variation diagram for the Wadi Nugrus lamprophyre dyke.

brown to black color and pleochroic from pale brown to dark brown.

Titanite is present as a large yellowish brown grain, whilst the ESEM analyses show its ideal composition of Ca, Ti and Si with some Fe and Ni present. Moreover, atacamite occurs as diagnostic crust-like aggregates or massive grains of deep green color. The ESEM analyses show that applicable amounts of Cu and Fe are also detected in the analyses. However, rutile is present with red color and shows a substitution of Ti by Fe and Ni.

Conclusions

Wadi Nugrus, varying in thickness from 0.5 to 1.5 m and up to 3 km in length, and cuts porphyritic biotite granites.

(2) Rounded to sub-rounded, porphyritic and zoned ocelli with radiate or brush-like shapes are generally common and represent physical traps for mineralization. The ocellar features are interpreted to represent late stage magmatic segregation or magmatic crystallization involving two immiscible magmatic liquids.

(3) The major and trace elements of the studied shoshonitic lamprophyre are all relatively homogeneous. The maximum Ni content of the studied rocks (for example, 136 ppm) is quite low in comparison to the common mantle magmas with similar Mg numbers (Le Maitre, 1989), whereas the Cr contents of the lamprophyre (27 to 308 ppm) fall in the range expected for primitive mantle magmas (50 to 350 ppm). It is thus clear, that the geochemical characteristics of the lamprophyre reflect the nature of the mantle source region.

(4) The Nugrus lamprophyre dyke is characterized by a high $K_2O + Na_2O$ content (4.00 to 9.10%), a high K_2O/Na_2O ratio (0.13 to 1.24) and a low TiO_2 content (0.85 to 0.99%). Moreover, they display the typical geochemical signatures of the K-rich magma, that is, low TiO_2 , low K_2O/Al_2O_3 and high LILE/HFSE ratios.

(5) The Abu- Rusheid NNW-SSE lamprophyre dyke (perpendicular to Nugrus ENE-WSW dyke) is mantle derived with high temperature and is rich in volatiles (CO_2 and P_2O_5) (Ibrahim et al., 2007). The supplied heat could liberate uranium from the biotite granite, as well as accessories (zircon, fluorite and allanite). The solution carrying uranium when cooled off or subjected to reducing conditions might lead to the formation of secondary uranium minerals in the presence of other anion and cation (autunite and uranophane). Excess uranium may be fixed by either adsorption on kaolinite, Fe-oxides and hydroxides or filling box works (ocelli) and sheared lamprophyre dyke. The later act as a physical (boxworks) or chemical (clay minerals) traps polymetallic mineralization (Ibrahim et al., 2007).

(6) The Abu- Rusheid mineralized NNW-SSE lamprophyre dyke which cross-cuts the hot cataclastic rocks, stopped at Nugrus ENE-WSW lamprophyre dyke. So, most of the migrated mineralization (base metals: nickel, copper, molybdenum and pyrite), associated with rutile, zircon, zincite, atacamite, fluorite, titanite and allanite from hot cataclastic rocks along the shear zone toward SSE direction, were accumulated at the wall zone of

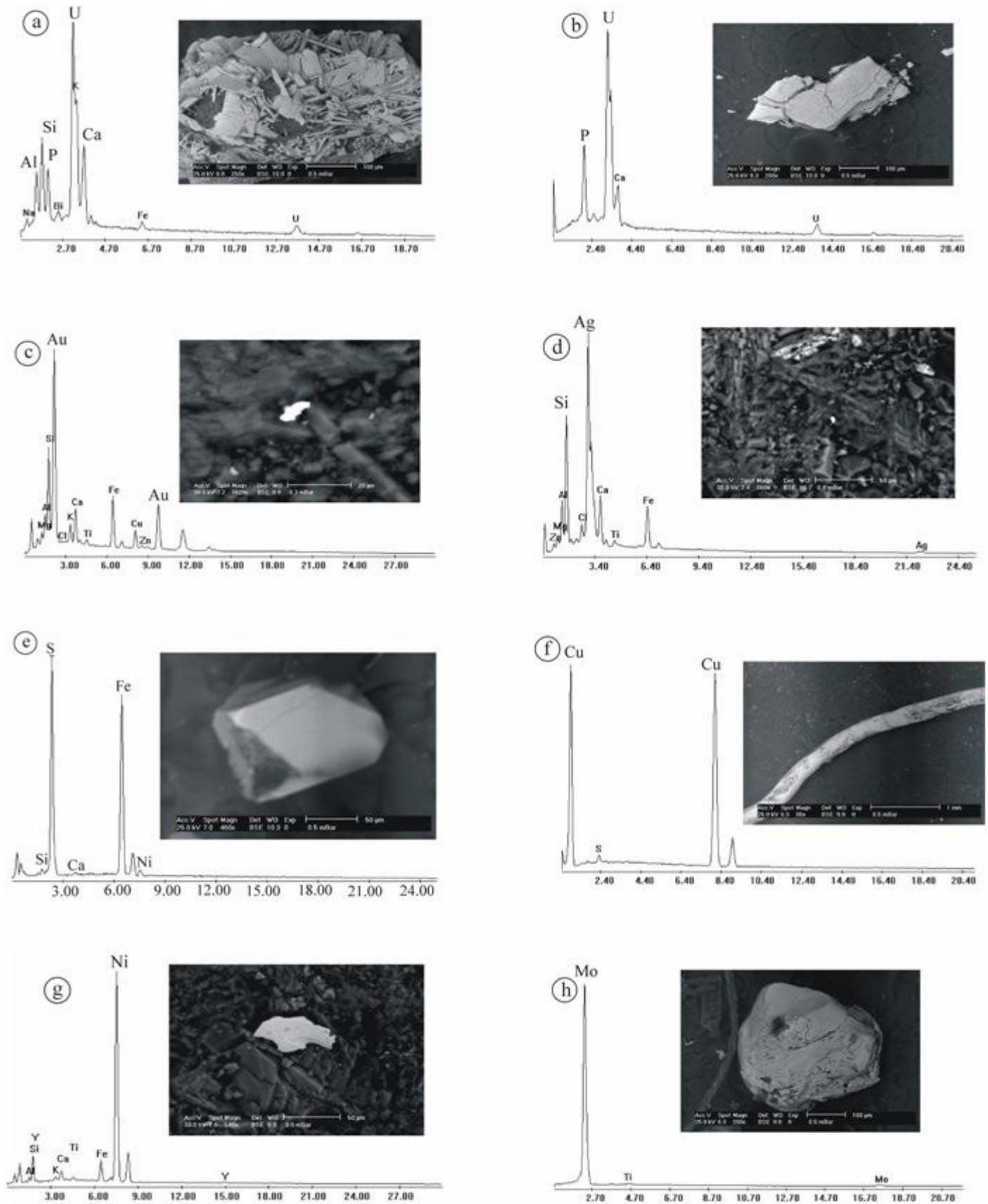


Figure 7. ESEM image showing (a) uranophane, (b) autunite, (c) gold, (d) silver, (e) pyrite, (f) copper, (g) nickel and (h) molybdenum.

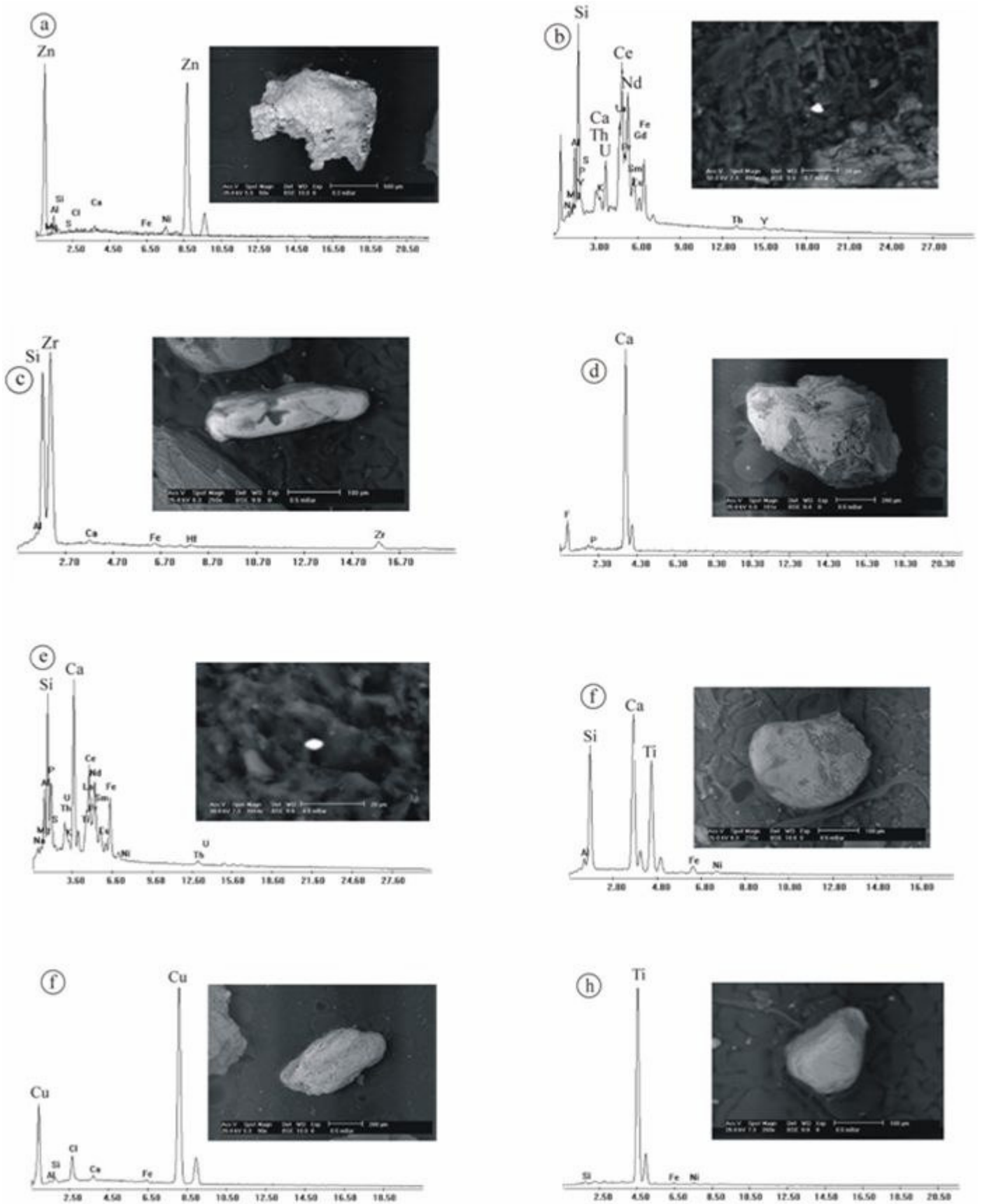


Figure 8. ESEM image showing (a) zincite, (b) REEs silicates, (c) zircon, (d) fluorite, (e) allanite, (f) titanite, (g) atacamite and (h) rutile.

Table 2. Results of the mineral assemblage in lamprophyre and Nugrus lamprophyre dyke, Southeastern Desert, Egypt.

Primary minerals		Supergene minerals		Secondary minerals	
Minerals	Composition	Minerals	Composition	Minerals	Composition
Gold	Au	Zincite	ZnO	Rutile	TiO ₂
Silver	Ag	Atacamite	Cu ₂ Cl(OH) ₃	Zircon	ZrSiO ₄
Nickel	Ni	Autunite	Ca(UO ₂)(PO ₄) ₂ .8H ₂ O	Fluorite	CaF ₂
Pyrite	FeS ₂	Uranophane	Ca.2U ₃ O ₂ .SiO ₂ .6H ₂ O	Titanite	CaTiSiO ₅
Molybdenum	Mo			Allanite	
Carbon	C			REE silicate	

Nugrus ENE-WSW lamprophyre dyke.

REFERENCES

- Berry LGM, Mason B, Dietrich RV (2000). Mineralogy. CBS Publishers and Distributors, New Delhi, India. p. 561.
- Cesborn F, Idefonse P, Sichere MD (1993). New mineralogical data on uranophane and B-Uranophane: *Ged. Magazine*, 57: 301-308.
- Cooper AF (1979). Petrology of ocellar lamprophyres from western Otago, Newzealand. *J. Petrol.*, 20: 139-163.
- Deer WA, Howie RA, Zussman J (1992). Rock forming minerals. Longman Group (FE) Ltd., Hong Kong, p. 696.
- Eby GN (1980). Minor and trace element partitioning between immiscible ocelli groundmass pairs from lamprophyre dykes and sills, Monteregain Hills petrographic province, Queec. *Contrib. Mineral. Petrol.*, 75: 269-278.
- Heinrich EW (1956). Microscopic petrology. McGraw-Hill Company, Inc., p. 295.
- Ibrahim IH, Ibrahim ME (2007). Comparative study between some uraniferous volcanic rocks, Eastern Desert, Egypt. The 10th International Mining, petroleum, and Metallurgical engineering Conference, March 6-8: 56-70.
- Ibrahim ME, Abd El-Wahed AA, Rashed MA, Khaleal FM, Mansour GM, Watanabe K (2007). Comparative study between alkaline and calc-alkaline lamprophyres in Abu Rusheid area, South Eastern Desert, Egypt. The 10th International Mining, petroleum, and Metallurgical engineering Conference, March 6-8: 99-115.
- Ibrahim ME, El Tokhi MM, Saleh GM, Rashed MA (2006). Lamprophyre bearing-REEs South Eastern Desert, Egypt. The 7th International Conference on Geochemistry, Alexandria University. pp. 12-38.
- Ibrahim ME, Saleh GM, Amer T, Mahmoud FO, Abu El Hassan AA, Ibrahim IH, Aly MA, Azab MS, Rashed MA, Khaleal FM, Mahmoud MA (2004). Uranium and associated rare metals potentialities of Abu Rusheid brecciated shear zone II, Southeastern Desert, Egypt. (Internal report).
- Kerr PF (1977). Optical mineralogy. 4th Ed., McGraw-Hill Book Inc, p. 492.
- Le Maitre RW (1989). A classification of igneous rocks and glossary of terms: Recommendations of the International Union of Geological Sciences, Subcommittee on the Systematics of Igneous Rocks. Blackwell, Oxford, p. 193.
- Loyd FE, Arima A, Adgar AD (1985). Partial melting of a phlogopite clinopyroxenite nodule from south-west Uganda: an experimental study bearing on the origin of highly potassic continental rift volcanics. *Contrib. Mineral. Petrol.*, 91: 321-329.
- Philpots AR (1976). Silicate liquid immiscibility: its probable extent and petrogenetic significance. *Am. J. Sci.*, 276: 1147-1177.
- Ramdohr P (1969). The ore minerals and their intergrowths. Pergamon, London, pp. 779-792
- Rock NMS (1987). The nature and origin of lamprophyres: an overview. In: Fitton, J. G. and Upton, B. G. J. (Eds.), alkaline igneous rocks. *Geol. Soc. London, Sp. Publ.*, 30: 191-226.
- Turner FJ (1953). Nature and dynamic interpretations of deformation lamellae in calcite of three marbles. *Am. J. Sci.*, 25: 276-298.